JACS
JOURNAL OF THE AMERICAN CHEMICAL SOCIETY

Article

pubs.acs.org/JACS

# Immobilizing Extremely Catalytically Active Palladium Nanoparticles to Carbon Nanospheres: A Weakly-Capping Growth Approach

Qi-Long Zhu,[†] Nobuko Tsumori,[†,‡] and Qiang Xu*[,†]

[†]National Institute of Advanced Industrial Science and Technology (AIST), Ikeda, Osaka 563-8577, Japan

[‡]Toyama National College of Technology, 13, Hongo-machi, Toyama, 939-8630, Japan

Supporting Information

**ABSTRACT:** Ultrafine palladium nanoparticles (Pd NPs) supported on carbon nanospheres have been successfully synthesized using a facile methanol-mediated weakly-capping growth approach (WCGA) with anhydrous methanol as a mild reductant and a weakly capping agent. The Pd NPs show exceedingly high catalytic activity for 100% selective dehydrogenation of aqueous formic acid (FA) at ambient temperatures. The small size and clean surface of the Pd NPs greatly improve the catalytic properties of the as-prepared catalyst, providing an average rate of CO-free $H_2$ generation up to 43 L $H_2$ $g_{Pd}^{-1}$ $min^{-1}$ and a turnover frequency of 7256 $h^{-1}$ at 60 °C. These values are much higher than those obtained even with the most active catalyst reported thus far for heterogeneously catalyzed dehydrogenation of FA. This remarkably facile and effective methanol-mediated WCGA provides a powerful entry into ultrafine metal NPs with clean surface to achieve enhanced performance. Moreover, the catalytic results open up new avenues in the effective applications of FA for hydrogen storage.

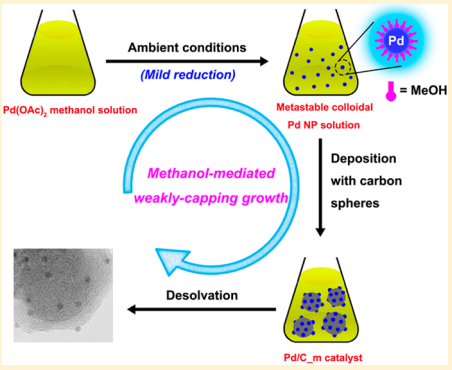


## INTRODUCTION

Ultrafine metal nanoparticles (NPs) are of fundamental interest because of their unique catalytic properties, which in turn are attributed to their high surface-to-atom ratio and an abundance of edge and corner atoms.[1] Since small metal NPs tend to aggregate due to their high surface energy, the synthesis of ultrafine NPs remains a challenge.[2] The recently reported colloidal methods involving coating the metal NPs with an outer shell of organic capping agents help in minimizing the agglomeration of metal NPs.[3] However, the exposed surface of the nanocatalysts is often contaminated by the chemical interactions between the capping agent molecules and the metal surface. On the other hand, owing to the lack of efficient ways to control the nucleation and growth of metal NPs, it is difficult to deposit ultrafine NPs on the solid supports. It has been found that a combination of high dispersion and clean metal surface of metal nanoparticles plays a crucial role in enhancing the catalytic activity of metal NPs.[4] For catalytic applications, the development of general and facile methods to obtain uncapped metal NPs with high dispersion is highly desirable.

Hydrogen is a renewable and environmentally promising energy carrier for future fuel cell applications because it possesses a high energy density and only affords a clean exhaust product, i.e., water vapor.[5] Formic acid (FA), a nontoxic and stable liquid under ambient conditions with a gravimetric hydrogen content of 4.4 wt %, has been identified as a secure and convenient carrier of hydrogen and could be well compatible with the existing infrastructures used for gasoline and diesel.[6] Particularly noteworthy is that FA has a high volumetric hydrogen density of 53 g $L^{-1}$, which exceeds the 2017 target of 40 g $L^{-1}$ for on-board hydrogen storage updated recently by the U.S. Department of Energy (DOE).[7] Moreover, modern industrial biomass processes and catalytic reduction of $CO_2$ with $H_2$ can produce FA on a large scale and at low cost.[8] Therefore, the efficient and selective conversion of liquid FA into $H_2$ and $CO_2$ under mild conditions, without CO generation, will enable the use of FA as an ideal hydrogen carrier.

Currently, Pd and Pd-based nanomaterials are the most widely used catalysts for $H_2$ generation from FA systems.[9] However, the activities and selectivities of these catalysts are still far from those required for practical applications. Moreover, the procedures presently used for the synthesis of catalysts generally involve multiple steps and strictly controlled reaction conditions, including inert gas protection, heating, and post-processing, greatly hindering their use in practical applications. Thus, a simple and facile strategy that allows easy control of the nucleation and growth of metal nanocatalysts with distinguished performance for FA dehydrogenation under ambient conditions is vital for practical hydrogen storage.

Herein, we report a facile methanol-mediated weakly-capping growth approach (WCGA) to prepare a special colloidal Pd NP solution, where anhydrous methanol acts not only as the solvent for the growth of Pd NPs but also as a mild reductant and a weakly capping agent to control the nucleation and

**Received:** June 29, 2015
**Published:** August 31, 2015





DOI: 10.1021/jacs.5b06707
J. Am. Chem. Soc. 2015, 137, 11743−11748

prevent the aggregation of the dispersed ultrafine Pd NPs. The Pd NPs weakly capped by methanol molecules can be immobilized on a carbon support to afford a stable surfactant-free catalyst, which exhibits high activity for complete and efficient $H_2$ production without CO impurity from aqueous FA under mild conditions. The resulting catalyst affords the highest turnover frequency (TOF; 7256 $h^{-1}$ at 60 °C) for the selective decomposition of FA in heterogeneous systems. The small size and clean surface of the naked Pd NPs should account for their excellent catalytic properties.

## EXPERIMENTAL SECTION

**Chemicals and Materials.** All chemicals were commercial and used without further purification. Palladium(II) acetate ($Pd(OAc)_2$, Wako Pure Chemical Industries, Ltd., >98%), potassium tetrachloropalladate ($K_2PdCl_4$, Wako Pure Chemical Industries, Ltd., >97%), sodium borohyride (SB, $NaBH_4$, Sigma-Aldrich, 99%), Vulcan XC-72R (Carbon, specific surface area = 240 $m^2$ $g^{-1}$, Cabot Corp., USA), formic acid (FA, HCOOH, Kishida Chemicals Co. Ltd., >98%), sodium formate dehydrate (SF, HCOONa, Sigma-Aldrich, 99.5%), acetone (Kishida Chem. Co., >99.5%), anhydrous methanol (MeOH, Kishida Chem. Co., >99.8%), and formaldehyde solution (HCHO, Wako Pure Chemical Industries, Ltd., 37% in water; it contains 5−10% of methanol as a stabilizer), poly(*N*-vinyl-2-pyrrolidone) K30 (PVP, $(C_6H_9NO)_n$, $M_w$ = av. 40000, Tokyo Chemical Industry Co., Ltd.) were used as received. Deionized water with a specific resistance of 18.2 MΩ·cm was obtained by reverse osmosis followed by ion-exchange and filtration (RFD 250NB, Toyo Seisakusho Kaisha, Ltd., Japan).

**Characterization of the Catalysts.** Laboratory powder X-ray diffraction (PXRD) patterns were collected for samples on Rigaku Ultima IV X-ray diffractometer using Cu $K_\alpha$ radiation ($\lambda$ = 0.15406 nm) (40 kV, 40 mA). The surface area measurements were performed with $N_2$ adsorption/desorption isotherms at liquid nitrogen temperature (77 K) using automatic volumetric adsorption equipment (Belsorp-max) after dehydration under vacuum at 120 °C for 12 h. The metal contents of the catalysts were analyzed using ICP-OES on Thermo Scientific iCAP6300. X-ray photoelectron spectroscopic (XPS) measurements were conducted on a Shimadzu ESCA-3400 X-ray photoelectron spectrometer using a Mg K$\alpha$ source (10 kV, 10 mA). The argon sputtering experiments were carried out under the conditions of background vacuum of 3.2 × $10^{-6}$ Pa, sputtering acceleration voltage of 2 kV and sputtering current of 10 mA. The charging potentials of the catalyst samples were corrected by setting the binding energy of the adventitious carbon (C 1s) at 284.6 eV. The transmission electron microscopy (TEM) and high-angle annular dark-field scanning TEM (HAADF-STEM) images were recorded on TECNAI $G^2$ F20 with operating voltage at 200 kV equipped with energy-dispersive X-ray detector (EDX). The gas generated from the decomposition of FA was analyzed by GC-8A TCD (molecular sieve 5A, Ar as carrier gas) and GC-8A TCD (Porapack N, He as carrier gas) analyzers (Shimadzu), which was collected after purging the reactor with argon three times. The detection limit was below 5 ppm for CO. The components of the liquid sample collected after reduction were determined based on authentic samples by GC-2014 FID analyzers (Shimadzu) assembled with DB-FFAP 30 m column.

**Synthesis of Pd/C_m Catalyst.** The supported Pd nanocatalyst was synthesized by using a facile methanol-mediated WCGA with the anhydrous methanol as the mild reductant. Typically, 225 mg of $Pd(OAc)_2$ was dissolved in 300 mL of anhydrous methanol in a beaker under stirring with exposure to ambient light. The initial pale yellow solution progressively darkened, suggesting the formation of the Pd colloidal nanoparticles. After continuous stirring for 15 min, 1.0 g of Vulcan XC-72R carbon powder was added and mixed for another 30 min for depositing the Pd nanoparticles. Subsequently, the solvent and unreduced precursor were removed by centrifuging. The collected solid was washed with anhydrous methanol twice and then dried under vacuum at room temperature to give the Pd/C_m catalyst.

For comparison, Pd/C_e and Pd/C_p catalysts were also prepared following the same synthetic procedures as that for Pd/C_m, except that ethanol and *n*-propanol were used instead of methanol, respectively.

**Syntheses of $Pd^{2+}$/C and Pd/C_*in situ*.** The $Pd^{2+}$/C precatalyst was prepared following the same synthetic procedure as that for Pd/C_m catalyst, except that acetone was used as the solvent instead of methanol. Pd/C_*in situ* was *in situ* generated when adding $Pd^{2+}$/C into the FA/SF solution under the catalytic conditions for FA dehydrogenation.

**Syntheses of Pd/C_SB and Pd/PVP-C_SB.** 100 mg of Vulcan XC-72R carbon powder (and 20 mg PVP for Pd/PVP-C_$NaBH_4$) was ultrasonically dispersed in 4 mL of water and subsequently mixed with an aqueous solution of $K_2PdCl_4$ (0.30 M, 0.20 mL). The resulted aqueous suspension was further homogenized under sonication condition for 30 min. Then, 20 mg of $NaBH_4$ dissolved in 1.0 mL water was added into the above suspension under vigorous stirring. The mixture was stirred for another 30 min at room temperature for fully depositing the metallic nanoparticles onto the support. Finally, the solid was collected by centrifuging and washed with deionized water three times and then dried under vacuum at room temperature.

*Procedure for the Decomposition of FA.* Reaction apparatus for measuring the $H_2$−$CO_2$ evolution from FA decomposition is the same as previously reported.[9b] In general, a mixture of the as-prepared Pd/C_m catalyst (100 mg) and distilled water (2 mL) was placed in a two-necked round-bottomed flask (30 mL), which was placed in a water bath at a preset temperature (30−60 °C) under ambient atmosphere. A gas buret filled with water was connected to the reaction flask to measure the volume of released gas (lab temperature kept constant at 25 °C during measurements). The reaction started when 1.5 mL of the mixed aqueous solution containing FA and SF (6.0 M) was injected into the mixture using a syringe. The volume of the evolved gas was monitored by recording the displacement of water in the gas buret.

*Durability Testing of the Catalysts.* For testing the durability of the as-prepared Pd/C_m catalyst, 0.34 mL of pure FA (9.0 mmol) was subsequently added into the reaction flask after the completion of the first-run decomposition of FA. Such test cycles of the catalyst for the decomposition of FA were carried out for 5 runs at 60 °C by adding aliquots of pure FA.

*Stability of the Catalysts.* After the reaction, the catalyst was separated from the reaction solution by centrifuging and washing with water and dried under vacuum at room temperature for the XPS, PXRD, and TEM analyses.

**Calculation Methods.** The TOF reported here is an apparent TOF value based on the number of Pd atoms in catalyst, which is calculated from the time of half-completion of gas generation and the equation as follows:

$$\mathrm{TOF} = \frac{P_{\mathrm{atm}} V_{\mathrm{gas}}/RT}{2 n_{\mathrm{Pd}} t} \quad (1)$$

where $P_{atm}$ is the atmospheric pressure (101325 Pa), $V_{gas}$ is the generated volume of $H_2$−$CO_2$ gas at the time of half-completion of gas generation, $R$ is the universal gas constant (8.3145 $m^3$ Pa $mol^{-1}$ $K^{-1}$), $T$ is the room temperature (298 K), $n_{Pd}$ is the total mole number of Pd atoms in catalyst, and $t$ is the time of half-completion of gas generation.

## RESULTS AND DISCUSSION

The facile methanol-mediated WCGA adopted for the synthesis of ultrafine Pd NPs supported on carbon is shown in Scheme 1. Under ambient conditions, $Pd(OAc)_2$ (1.0 mmol) dissolved in anhydrous methanol (300 mL) was gradually reduced, as evidenced by the progressive darkening of the solution color, leading to the formation of a suspension of colloidal Pd NPs. The colloidal Pd NPs, which may be stabilized by the weak capping of methanol molecules, can remain stable in methanol solution for more than 1 h without aggregation. Before their


DOI: 10.1021/jacs.5b06707
J. Am. Chem. Soc. 2015, 137, 11743−11748

**Scheme 1. Schematic Representation for the Preparation of Pd/C_m Catalyst via a Methanol-Mediated WCGA**

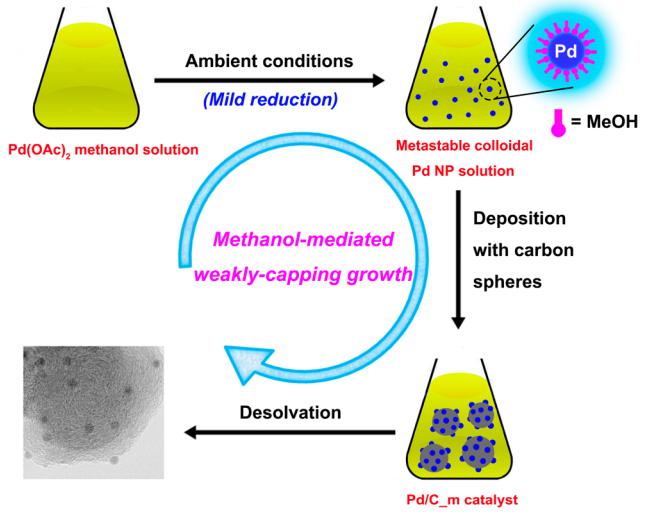


aggregation, the methanol-mediated Pd NPs were deposited on carbon nanospheres (Vulcan XC-72R, 1.0 g), affording a stable Pd/C_m catalyst, while the unreduced $Pd^{2+}$ ions were removed by centrifuging and washing. The Pd loading in the as-prepared catalyst was determined to be 6.0 wt % by ICP. The as-prepared Pd/C_m possesses a clean and highly active Pd surface, in contrast to the catalysts prepared by previously reported methanol reduction approaches involving heating and the use of strong capping agents.[10]

Remarkably, the as-prepared Pd/C_m can serve as an efficient catalyst for the complete and selective decomposition of FA into $H_2$ and $CO_2$. The released gaseous mixture was measured volumetrically, and its composition was analyzed by gas chromatography (GC). With 100 mg of the catalyst, 450 mL of the gaseous mixture was released in 1.75 min from the aqueous FA-SF system (FA:SF = 1:1, $n_{Pd}/n_{FA}$ = 0.006) at 60 °C (Figure 1a). The excess volume over the theoretical value (432 mL) from FA decomposition can be attributed to $H_2$ generation from the hydrolysis of a small amount of SF in this system. The exclusive formation of $H_2$ and $CO_2$ without CO contamination, which is critical for proton exchange membrane (PEM) fuel cell applications, was confirmed by GC analyses (Figures S3 and S4). It is worth noting that the as-prepared Pd/C_m catalyst provided an exceptional TOF of 7256 $h^{-1}$ (Figure 1b), which is much higher than that obtained with the most active heterogeneous catalyst reported thus far (Table S1).[9h] The average rate of $H_2$ evolution was determined to be 43 L $H_2$ $min^{-1}$ $g_{Pd}^{-1}$, which corresponds to a high energy density of 58 W $min^{-1}$ $g_{Pd}^{-1}$. Owing to the low operating temperature, the hydrogen release of this system can be driven by the waste heat of a standard PEM fuel cell without additional heat treatment.[6i] To the best of our knowledge, only a few solid catalysts reported so far for FA decomposition can maintain their initial high activities for the overall reaction time.[9e,11] The aforementioned trend may be explained by the fact that these catalysts show high catalytic selectivity, and thus, the undesired dehydration pathway (HCOOH → $H_2O$ + CO) can be strictly controlled to protect them against poisoning. In order to test the stability of the as-prepared Pd/C_m catalyst, the dehydrogenation reaction was carried out for five runs, and only a slight decrease in activity was observed (Figure S8),

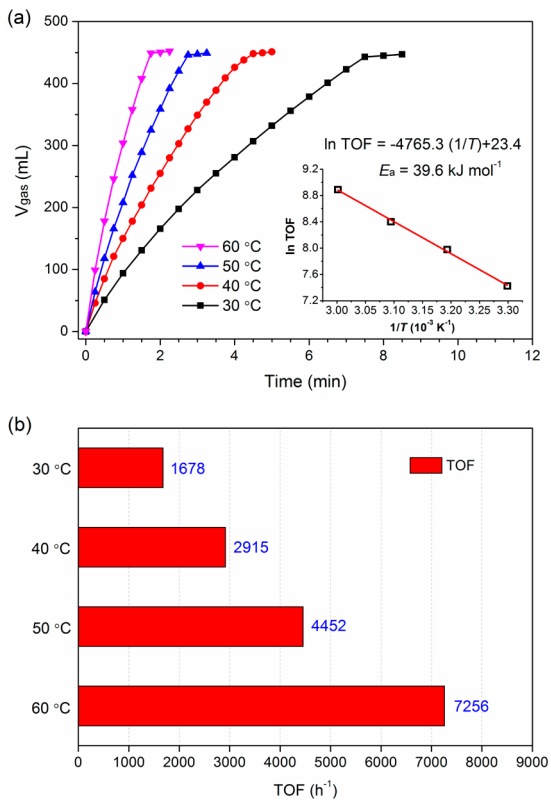


**Figure 1.** Temperature dependence of (a) gas evolution from the aqueous FA-SF solution in the presence of as-prepared Pd/C_m catalyst and (b) the corresponding TOF values for $H_2$ evolution (FA:SF = 1:1, $n_{Pd}/n_{FA}$ = 0.006). Inset of (a): Arrhenius plot (ln(TOF) vs $1/T$).

reliably indicating the high durability and stability of the as-prepared catalyst for FA decomposition.

The effect of FA/SF molar ratio on the performance of the as-prepared Pd/C_m catalyst was investigated. Increasing the molar percentage of SF induced a rapid increase in the activity of Pd/C_m for FA dehydrogenation until a maximum value was achieved at 50%; lower FA/SF ratios led to negligible changes in the catalytic activity (Figure S5). Typically, very slow gas generation was observed for pure FA, which further confirms the important role of SF as a catalyst promoter. The formate additive is believed to induce a favorable adsorption configuration of FA molecules on the metal surface to accelerate the kinetics of FA decomposition and/or to act as an active intermediate (e.g., the Pd-formate species) to facilitate $CO_2$ production.[9f,12] Recently, several reports have described the feasibility of using the formate/bicarbonate redox couple for hydrogen storage.[13] The as-prepared Pd/C_m catalyst was also active for the direct hydrolysis of aqueous SF, though the activity was lower than that for the dehydrogenation of the FA-SF system (Figure S6). Moreover, the hydrogen release rate was strongly dependent on the reaction temperature (Figure 1). Remarkably, the as-prepared catalyst showed significant catalytic performance, with a high TOF of 1678 $h^{-1}$, even at a low temperature of 30 °C. The apparent activation energy ($E_a$) of this reaction estimated within the temperature range of 30–60 °C was 39.6 kJ $mol^{-1}$ (inset of Figure 1a), which is lower than most of the previously reported values.[9] Consequently, in the presence of the as-prepared Pd/C_m


DOI: 10.1021/jacs.5b06707
J. Am. Chem. Soc. 2015, 137, 11743–11748

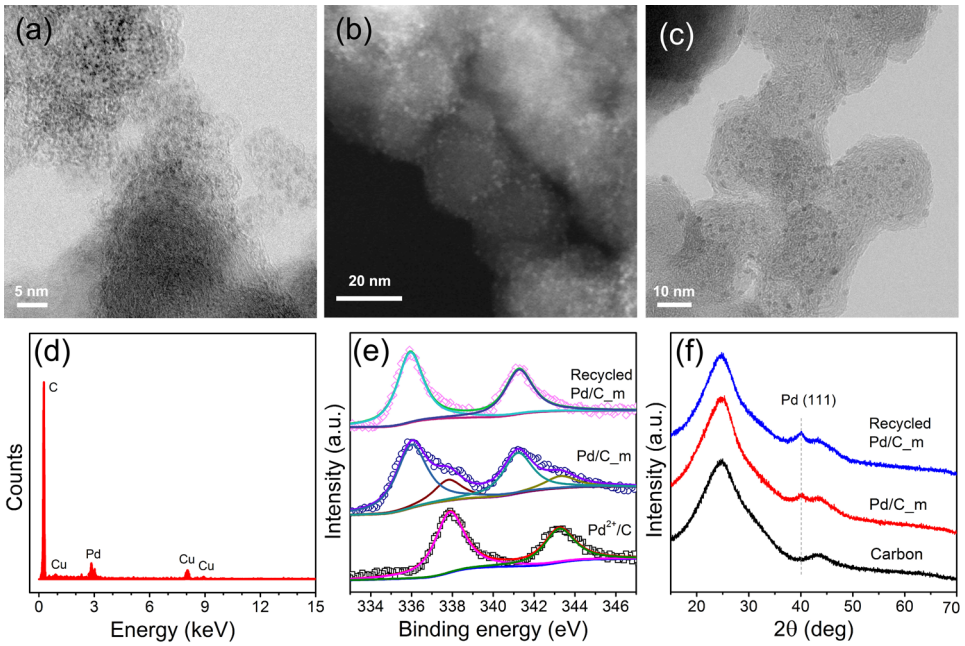


**Figure 2.** (a) TEM, (b) HAADF-STEM images and (d) EDS pattern of the as-prepared Pd/C_m catalyst, (c) TEM image of the Pd/C_m catalyst recycled from the reaction solution, (e) XPS spectra of Pd element in the as-prepared and recycled Pd/C_m, and $Pd^{2+}$/C, and (f) PXRD patterns of carbon support, as-prepared and recycled Pd/C_m.

catalyst, a large CO-free $H_2$−$CO_2$ stream can be readily achieved from aqueous FA at convenient temperatures.

The structure and morphology of the as-prepared Pd/C_m catalyst before and after catalysis were analyzed. The TEM and HAADF-STEM images of the as-prepared Pd/C_m catalyst show that the average particle size of the highly dispersed Pd NPs immobilized on carbon nanospheres is 1.4 ± 0.3 nm (Figures 2a,b and S2a). Compared with the carbon support, the amount of nitrogen adsorption decreased appreciably after the deposition of Pd NPs on the carbon support (Figure S1), suggesting that the mesopores of the carbon nanospheres could be partially occupied by the ultrafine Pd NPs. XPS analyses were conducted to examine the surface chemistry of the catalysts (Figure 2e). Four major contributions were identified from the Pd 3d spectrum of the as-prepared Pd/C_m catalyst. The contributions at ca. 336.0 and 341.2 eV could be assigned to metallic Pd. Notably, two additional small contributions at ca. 337.8 and 343.4 eV indicated that in the as-prepared catalyst, a small amount of Pd exists in the form of $Pd(OAc)_2$ rather than as Pd(0), as confirmed by the similar binding energy of $Pd^{2+}$ cations. The $Pd^{2+}$/C sample for verification was prepared by depositing the precursor on carbon in a nonreductive acetone solution. Therefore, in the methanol-mediated WCGA, most of the $Pd^{2+}$ ions can be reduced by MeOH, while the presence of $Pd(OAc)_2$ in the as-prepared catalyst is ascribed to the incomplete reduction with MeOH and the adsorption in carbon pores. In the XRD patterns of the as-prepared Pd/C_m catalyst, only a weak and broad peak at around 40.0° corresponding to Pd(II) was detected (Figure 2f), further confirming the formation of very small Pd NPs.

The TEM image of the catalyst collected from the reaction solution suggests that the high dispersion of the Pd NPs can be maintained during the reaction and that the average particle size of 1.7 ± 0.5 nm (Figures 2c and S2b) is consistent with the XRD results (Figure 2f). However, statistical analysis revealed a slightly larger average particle size and broader size distribution in the used catalyst as compared to the as-prepared catalyst (Figure S2). This difference may be because the *in situ* reduction of residual $Pd^{2+}$ cations adsorbed in the pores of carbon by the moderate reductant FA/SF affords larger nanoparticles[14] and/or the preformed Pd NPs agglomerate slightly due to ripening during the catalytic process. The disappearance of the small contributions attributed to $Pd^{2+}$ cations further demonstrates the complete reduction of $Pd^{2+}$ to $Pd^0$ in the recycled catalyst (Figure 2e). Besides, the comparison of XRD, XPS, and TEM results before and after catalysis suggests that the crystalline, surface electronic structure and morphology of Pd(0) in Pd/C_m were maintained during catalysis (Figure 2e,f).

For further insights into the methanol-mediated weakly-capping growth of Pd NPs in MeOH, we monitored the color changes of the methanol solution of the precursor. As shown in Figure 3a, the dissolution of $Pd(OAc)_2$ in MeOH gave a clear solution, whose color progressively changed from pale yellow to black within 60 min under ambient conditions. Under strictly anhydrous conditions, a faster color change was observed (the solution turned black in ca. 30 min). After reduction, the clear liquid separated from the reaction mixtures of Pd/C_m was tested by GC, and it was found that FA and formaldehyde were formed as intermediates from MeOH during the reduction processes (Figure 3c), further indicating the weakly reducing capacity of MeOH. Because the as-prepared Pd/C_m catalyst was inactive for the decomposition of FA in methanol solution at room temperature (Figure S9), the small amount of FA intermediate formed from MeOH could be detected here. In contrast, the attempted reduction of $Pd(OAc)_2$ by acetone was not successful (Figure 3b). As the reaction time has a significant effect on the degree of reduction, the amount of Pd NPs formed and subsequently deposited on carbon can be varied by changing the reduction/deposition time (7.5, 15, 30, and 60 min). According to ICP analysis, the Pd loading in the catalyst was increased with the stirring time after adding carbon powder


DOI: 10.1021/jacs.5b06707
J. Am. Chem. Soc. 2015, 137, 11743−11748

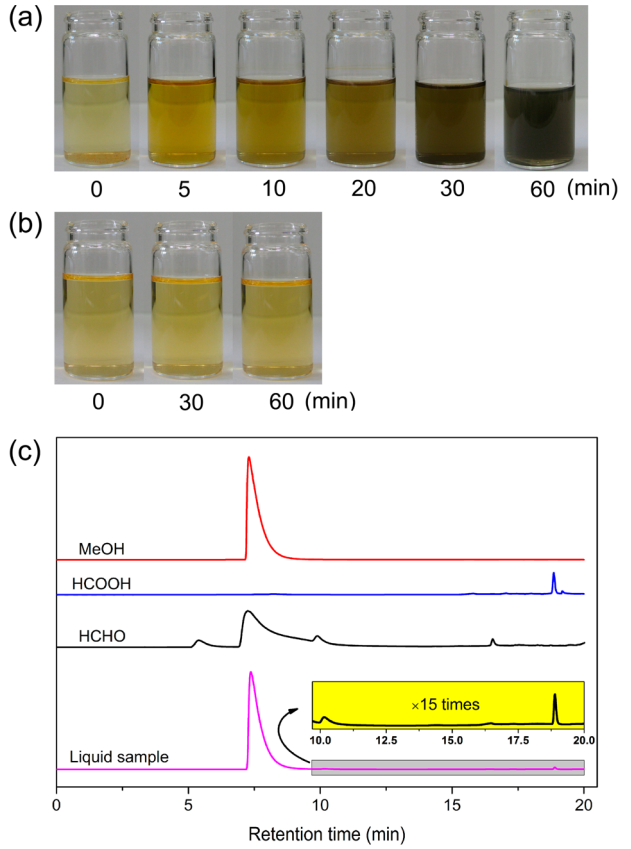


**Figure 3.** Time-progression color changes of the (a) methanol and (b) acetone solutions of $Pd(OAc)_2$ under ambient conditions for monitoring the formation of colloidal Pd NPs, and (c) GC-FID chromatograms of methanol, FA and formaldehyde as reference compounds, and the liquid separated from the reaction mixtures of Pd/C_m.

and reached a maximum value of 6.0 wt % in 30 min; further increase in the stirring time had little effect on the loading percentage (Table S2). Notably, the catalysts with different Pd loadings gave similar TOF values, probably because of the similar dispersion of Pd NPs (Figure S7).

Experiments were also performed to evaluate the weakly capping and reducing abilities of other alcohols, such as ethanol and *n*-propanol. Because of the stronger reducing ability of ethanol as compared to methanol, a slightly faster reduction process was observed, which was indicated by the faster darkening of the precursor solution. The Pd/C_e catalyst exhibited a slightly lower catalytic activity than that of Pd/C_m for the decomposition of FA (Figure S10). The much stronger reducing ability of *n*-propanol resulted in much faster darkening of the precursor solution, reflecting faster nucleation and, thus, slight aggregation of the Pd NPs. As a result, much lower activity was observed for the Pd/C_p catalyst (Figure S10).

To determine the significant effects of the dispersion and surfactant-free nature of Pd NPs on the catalytic activity for FA decomposition, both surfactant-free and surfactant-protected Pd/C catalysts were prepared using different methods. Compared to the case of the as-prepared Pd/C_m catalyst, a larger Pd particle size and broader size distribution ($3.2 \pm 0.5$ nm) were observed for Pd/C_*in situ* reduced from $Pd^{2+}$/C, by FA/SF (Figure S13a). On the other hand, reduction with $NaBH_4$ caused severe agglomeration of Pd in Pd/C_SB, with an increase in the Pd particle size to 4.0−10.0 nm (Figure S13b). As a result, the activities of both catalysts were much lower than that of the as-prepared Pd/C_m catalyst (Figure 4),

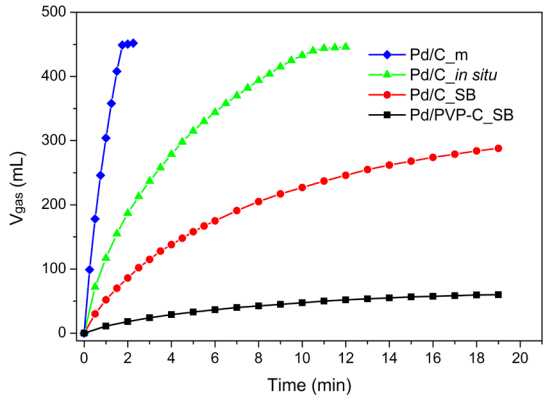


**Figure 4.** Comparison of the catalytic activities of the as-prepared Pd/C_m, Pd/C_*in situ*, Pd/C_SB, and Pd/PVP-C_SB catalysts for the dehydrogenation of FA (FA:SF = 1:1; FA, 9 mmol; catalyst, 100 mg).

indicating that the catalytic activity is highly dependent on the particle size of the metal NP. Moreover, in contrast to the excellent durability of Pd/C_m, more than half of the catalytic efficiency missed for Pd/C_*in situ* over the three runs (Figure S11). For the PVP-protected Pd/PVP-C_SB catalyst, surprisingly, despite the small Pd particle size (∼3.5 nm) (Figure S13c), only negligible activity was observed (Figure 4). The above-mentioned observations demonstrate that the protective surfactant molecules adsorbed around the metal surface significantly hinder the access of reactants to the active sites of Pd NPs and therefore have an adverse impact on the catalytic activity. Consequently, the combination of the small particle size and the surfactant-free nature of Pd NPs in the as-prepared Pd/C_m catalyst accounts for the observed high activity.

## CONCLUSIONS

In summary, surfactant-free monometallic Pd nanoparticles have been successfully immobilized on carbon nanospheres with good dispersion by using a facile methanol-mediated WCGA, wherein methanol serves as both a mild reductant and a weakly capping agent to control the nucleation and prevent the aggregation of colloidal Pd NPs. The Pd NPs show extremely high catalytic activity and selectivity for the dehydrogenation of FA under mild conditions, over which the highest reported TOF of 7256 $h^{-1}$ at 60 °C has been achieved with the as-prepared Pd/C_m catalyst for the heterogeneously catalyzed dehydrogenation of FA. The catalyst is believed to give a tremendous boost to the practical application of FA for chemical hydrogen storage. Meanwhile, the utilization of this facile and economical reduction approach to obtain and subsequently deposit ultrafine metal NPs on various solid supports is expected to open new routes for designing highly efficient nanocatalysts.

## ASSOCIATED CONTENT

### Supporting Information

The Supporting Information is available free of charge on the ACS Publications website at DOI: 10.1021/jacs.5b06707.

PXRD, BET, EDX for catalysts; additional results of catalytic FA dehydrogenation; durability and stability results of catalysts (PDF)



DOI: 10.1021/jacs.5b06707
J. Am. Chem. Soc. 2015, 137, 11743−11748

## AUTHOR INFORMATION


### Corresponding Author

*q.xu@aist.go.jp


### Notes

The authors declare no competing financial interest.

## ACKNOWLEDGMENTS

The authors are thankful to the editor and the reviewers for their valuable suggestions, Dr. Takeyuki Uchida for TEM measurements, and AIST and JSPS for financial support. Q.L.Z. thanks JSPS for postdoctoral fellowship.

## REFERENCES


(1) (a) Xie, Y.; Ding, K.; Liu, Z.; Tao, R.; Sun, Z.; Zhang, H.; An, G. *J. Am. Chem. Soc.* **2009**, *131*, 6648. (b) Li, X.-H.; Wang, X.; Antonietti, M. *Chem. Sci.* **2012**, *3*, 2170. (c) Wang, W.-N.; An, W.-J.; Ramalingam, B.; Mukherjee, S.; Niedzwiedzki, D. M.; Gangopadhyay, S.; Biswas, P. *J. Am. Chem. Soc.* **2012**, *134*, 11276. (d) Li, X.-H.; Antonietti, M. *Chem. Soc. Rev.* **2013**, *42*, 6593. (e) Cai, Y.-Y.; Li, X.-H.; Zhang, Y.-N.; Wei, X.; Wang, K.-X.; Chen, J.-S. *Angew. Chem., Int. Ed.* **2013**, *52*, 11822. (f) Hu, P.; Morabito, J. V.; Tsung, C.-K. *ACS Catal.* **2014**, *4*, 4409. (g) Zhu, Q.-L.; Xu, Q. *Chem. Soc. Rev.* **2014**, *43*, 5468.

(2) (a) Thanh, N. T. K.; Maclean, N.; Mahiddine, S. *Chem. Rev.* **2014**, *114*, 7610. (b) Vollmer, C.; Janiak, C. *Coord. Chem. Rev.* **2011**, *255*, 2039.

(3) (a) Crooks, R. M.; Zhao, M.; Sun, L.; Chechik, V.; Yeung, L. K. *Acc. Chem. Res.* **2001**, *34*, 181. (b) Lowe, A. B.; Sumerlin, B. S.; Donovan, M. S.; McCormick, C. L. *J. Am. Chem. Soc.* **2002**, *124*, 11562. (c) Roucoux, A.; Schulz, J.; Patin, H. *Chem. Rev.* **2002**, *102*, 3757. (d) Narayanan, R.; El-Sayed, M. A. *J. Phys. Chem. B* **2005**, *109*, 12663. (e) Lohse, S. E.; Murphy, C. J. *J. Am. Chem. Soc.* **2012**, *134*, 15607.

(4) (a) Kundu, P.; Nethravathi, C.; Deshpande, P. A.; Rajamathi, M.; Madras, G.; Ravishankar, N. *Chem. Mater.* **2011**, *23*, 2772. (b) Chen, X.; Wu, G.; Chen, J.; Chen, X.; Xie, Z.; Wang, X. *J. Am. Chem. Soc.* **2011**, *133*, 3693. (c) Aijaz, A.; Karkamkar, A.; Choi, Y. J.; Tsumori, N.; Rönnebro, E.; Autrey, T.; Shioyama, H.; Xu, Q. *J. Am. Chem. Soc.* **2012**, *134*, 13926. (d) Li, X.-H.; Wang, X.; Antonietti, M. *Chem. Sci.* **2012**, *3*, 2170. (e) Zhu, Q.-L.; Li, J.; Xu, Q. *J. Am. Chem. Soc.* **2013**, *135*, 10210. (f) Li, X.-H.; Cai, Y.-Y.; Gong, L.-H.; Fu, W.; Wang, K.-X.; Bao, H.-L.; Wei, X.; Chen, J.-S. *Chem. - Eur. J.* **2014**, *20*, 16732. (g) Guo, L.-T.; Cai, Y.-Y.; Ge, J.-M.; Zhang, Y.-N.; Gong, L.-H.; Li, X.-H.; Wang, K.-X.; Ren, Q.-Z.; Su, J.; Chen, J.-S. *ACS Catal.* **2015**, *5*, 388.

(5) (a) Schlapbach, L.; Zuttel, A. *Nature* **2001**, *414*, 353. (b) Murray, L. J.; Dinca, M.; Long, J. R. *Chem. Soc. Rev.* **2009**, *38*, 1294. (c) Eberle, U.; Felderhoff, M.; Schüth, F. *Angew. Chem., Int. Ed.* **2009**, *48*, 6608. (d) Hamilton, C. W.; Baker, R. T.; Staubitz, A.; Manners, I. *Chem. Soc. Rev.* **2009**, *38*, 279. (e) Graetz, J. *Chem. Soc. Rev.* **2009**, *38*, 73. (f) Yang, J.; Sudik, A.; Wolverton, C.; Siegel, D. J. *Chem. Soc. Rev.* **2010**, *39*, 656. (g) Kim, S. K.; Han, W. S.; Kim, T. J.; Kim, T. Y.; Nam, S. W.; Mitoraj, M.; Piekos, L.; Michalak, A.; Hwang, S. J.; Kang, S. O. *J. Am. Chem. Soc.* **2010**, *132*, 9954. (h) Demirci, U. B.; Miele, P. *Energy Environ. Sci.* **2011**, *4*, 3334. (i) Neiner, D.; Karkamkar, A.; Bowden, M.; Joon Choi, Y.; Luedtke, A.; Holladay, J.; Fisher, A.; Szymczak, N.; Autrey, T. *Energy Environ. Sci.* **2011**, *4*, 4187. (j) Yadav, M.; Xu, Q. *Energy Environ. Sci.* **2012**, *5*, 9698. (k) Teichmann, D.; Arlt, W.; Wasserscheid, P. *Int. J. Hydrogen Energy* **2012**, *37*, 18118. (l) Huang, Z.; Autrey, T. *Energy Environ. Sci.* **2012**, *5*, 9257. (m) Chen, H. M.; Chen, C. K.; Liu, R.-S.; Zhang, L.; Zhang, J.; Wilkinson, D. P. *Chem. Soc. Rev.* **2012**, *41*, 5654. (n) Dalebrook, A. F.; Gan, W.; Grasemann, M.; Moret, S.; Laurenczy, G. *Chem. Commun.* **2013**, *49*, 8735.

(6) (a) Joó, F. *ChemSusChem* **2008**, *1*, 805. (b) Fellay, C.; Dyson, P. J.; Laurenczy, G. *Angew. Chem., Int. Ed.* **2008**, *47*, 3966. (c) Enthaler, S.; von Langermann, J.; Schmidt, T. *Energy Environ. Sci.* **2010**, *3*, 1207. (d) Johnson, T. C.; Morris, D. J.; Wills, M. *Chem. Soc. Rev.* **2010**, *39*, 81. (e) Boddien, A.; Mellmann, D.; Gärtner, F.; Jackstell, R.; Junge, H.; Dyson, P. J.; Laurenczy, G.; Ludwig, R.; Beller, M. *Science* **2011**, *333*, 1733. (f) Grasemann, M.; Laurenczy, G. *Energy Environ. Sci.* **2012**, *5*, 8171. (g) Barnard, J. H.; Wang, C.; Berry, N. G.; Xiao, J. *Chem. Sci.* **2013**, *4*, 1234. (h) Myers, T. W.; Berben, L. A. *Chem. Sci.* **2014**, *5*, 2771. (i) Zhu, Q.-L.; Xu, Q. *Energy Environ. Sci.* **2015**, *8*, 478. (j) Chauvier, C.; Tlili, A.; Das Neves Gomes, C.; Thuery, P.; Cantat, T. *Chem. Sci.* **2015**, *6*, 2938.

(7) *Targets for Onboard Hydrogen Storage Systems for Light-Duty Vehicles*, U.S. Department of Energy, Office of Energy Efficiency and Renewable Energy, http://energy.gov/eere/fuelcells/downloads/doe-targets-onboard-hydrogen-storage-systems-light-duty-vehicles.

(8) (a) Jessop, P. G.; Joó, F.; Tai, C.-C. *Coord. Chem. Rev.* **2004**, *248*, 2425. (b) Federsel, C.; Boddien, A.; Jackstell, R.; Jennerjahn, R.; Dyson, P. J.; Scopelliti, R.; Laurenczy, G.; Beller, M. *Angew. Chem., Int. Ed.* **2010**, *49*, 9777. (c) Boddien, A.; Gärtner, F.; Federsel, C.; Sponholz, P.; Mellmann, D.; Jackstell, R.; Junge, H.; Beller, M. *Angew. Chem., Int. Ed.* **2011**, *50*, 6411. (d) Hull, J. F.; Himeda, Y.; Wang, W.-H.; Hashiguchi, B.; Periana, R.; Szalda, D. J.; Muckerman, J. T.; Fujita, E. *Nat. Chem.* **2012**, *4*, 383. (e) Moret, S.; Dyson, P. J.; Laurenczy, G. *Nat. Commun.* **2014**, *5*, 4017.

(9) (a) Zhou, X.; Huang, Y.; Liu, C.; Liao, J.; Lu, T.; Xing, W. *ChemSusChem* **2010**, *3*, 1379. (b) Gu, X.; Lu, Z.-H.; Jiang, H.-L.; Akita, T.; Xu, Q. *J. Am. Chem. Soc.* **2011**, *133*, 11822. (c) Tedsree, K.; Li, T.; Jones, S.; Chan, C. W. A.; Yu, K. M. K.; Bagot, P. A. J.; Marquis, E. A.; Smith, G. D. W.; Tsang, S. C. E. *Nat. Nanotechnol.* **2011**, *6*, 302. (d) Wang, Z.-L.; Yan, J.-M.; Ping, Y.; Wang, H.-L.; Zheng, W.-T.; Jiang, Q. *Angew. Chem., Int. Ed.* **2013**, *52*, 4406. (e) Zhu, Q.-L.; Tsumori, N.; Xu, Q. *Chem. Sci.* **2014**, *5*, 195. (f) Jiang, K.; Xu, K.; Zou, S.; Cai, W.-B. *J. Am. Chem. Soc.* **2014**, *136*, 4861. (g) Bi, Q.-Y.; Lin, J.-D.; Liu, Y.-M.; Du, X.-L.; Wang, J.-Q.; He, H.-Y.; Cao, Y. *Angew. Chem., Int. Ed.* **2014**, *53*, 13583. (h) Chen, Y.; Zhu, Q.-L.; Tsumori, N.; Xu, Q. *J. Am. Chem. Soc.* **2015**, *137*, 106. (i) Song, F.-Z.; Zhu, Q.-L.; Tsumori, N.; Xu, Q. *ACS Catal.* **2015**, *5*, 5141.

(10) (a) Kuhn, J. N.; Huang, W.; Tsung, C.-K.; Zhang, Y.; Somorjai, G. A. *J. Am. Chem. Soc.* **2008**, *130*, 14026. (b) Ornelas, C.; Diallo, A. K.; Ruiz, J.; Astruc, D. *Adv. Synth. Catal.* **2009**, *351*, 2147. (c) Xiao, C.; Maligal-Ganesh, R. V.; Li, T.; Qi, Z.; Guo, Z.; Brashler, K. T.; Goes, S.; Li, X.; Goh, T. W.; Winans, R. E.; Huang, W. *ChemSusChem* **2013**, *6*, 1915.

(11) Bi, Q.-Y.; Du, X.-L.; Liu, Y.-M.; Cao, Y.; He, H.-Y.; Fan, K.-N. *J. Am. Chem. Soc.* **2012**, *134*, 8926.

(12) (a) Wang, H.-F.; Liu, Z.-P. *J. Phys. Chem. C* **2009**, *113*, 17502. (b) Gao, W.; Keith, J. A.; Anton, J.; Jacob, T. *J. Am. Chem. Soc.* **2010**, *132*, 18377. (c) Peng, B.; Wang, H.-F.; Liu, Z.-P.; Cai, W.-B. *J. Phys. Chem. C* **2010**, *114*, 3102. (d) Joo, J.; Uchida, T.; Cuesta, A.; Koper, M. T. M.; Osawa, M. *J. Am. Chem. Soc.* **2013**, *135*, 9991. (e) Mori, K.; Dojo, M.; Yamashita, H. *ACS Catal.* **2013**, *3*, 1114.

(13) (a) Papp, G.; Csorba, J.; Laurenczy, G.; Joo, F. *Angew. Chem., Int. Ed.* **2011**, *50*, 10433. (b) Boddien, A.; Federsel, C.; Sponholz, P.; Mellmann, D.; Jackstell, R.; Junge, H.; Laurenczy, G.; Beller, M. *Energy Environ. Sci.* **2012**, *5*, 8907.

(14) Jaganathan, R.; Ghugikar, V. G.; Gholap, R. V.; Chaudhari, R. V.; Mills, P. L. *Ind. Eng. Chem. Res.* **1999**, *38*, 4634.




DOI: 10.1021/jacs.5b06707
*J. Am. Chem. Soc.* 2015, 137, 11743−11748